JCTC Journal of Chemical Theory and Computation

Article

Cite This: J. Chem. Theory Comput. 2019, 15, 5523−5531

pubs.acs.org/JCTC

Accuracy of Spin-Component-Scaled CC2 Excitation Energies and Potential Energy Surfaces

Attila Tajti* and Péter G. Szalay*

ELTE Eötvös Loránd University, Laboratory of Theoretical Chemistry, Pázmány Péter sétány 1/A, H-1117 Budapest, Hungary

Supporting Information

Benchmark calculations with the Spin-Component-Scaled CC2 variants SCS-CC2 and SOS-CC2 are presented for the electronically excited valence and Rydberg states of small- and medium-sized molecules. Besides the vertical excitation energies and excited state gradients, the potential energy surfaces are also investigated via scans following the forces that act in the Franck−Condon region. The results are compared to the regular CC2 ones, as well as higher level methods CCSD, CCSD(T)(a)*, and CCSDT. The results indicate that a large fraction of the flaws of CC2 revealed by earlier studies disappears if spin-component scaling is employed. This makes these variants attractive alternatives of their unscaled counterparts, offering competitive accuracy of vertical excitation energies of both valence and Rydberg type states and reliable potential energy surfaces, while also maintaining a low-power-scaling computational cost with the system size.

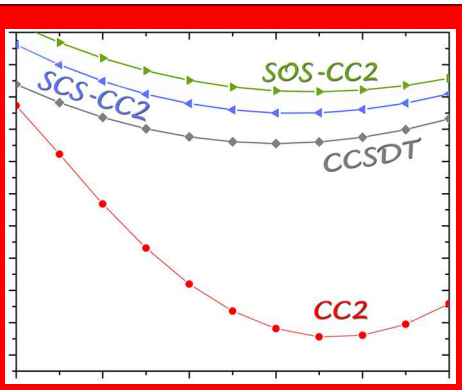

1. INTRODUCTION

The application of quantum chemical methods for electronically excited states is subject to wide scientific interest due to their role in spectroscopy, biological processes, photovoltaics, and many other fields. As these research areas are turning toward larger and larger molecules, efficient methods for theoretical characterization are warranted. Excited states are, however, generally more difficult to describe than the ground state, and many cost-effective computational approaches are unreliable or perform inconsistently for excited states. In the applications, the equation of motion (EOM)[1−3] or linear response (LR)[4−8] versions of coupled cluster (CC) theory[9−11] gained a high level of popularity in the past decade, thanks to their black-box applicability and reliability based mostly on their hierarchical structure.

As the excited state CC variants that account for the triple excitations are generally too expensive to be used for larger systems, lower-level approaches are mostly chosen, ones that scale with no more than the sixth, but preferably with the fifth or even fourth power of the system size: EOM-CCSD[1,2] and its approximations CC2,[7] EOM-CCSD(2),[12] partitioned EOM-MBPT(2),[13] and many others.

As the performance of such approximate methods is highly inconsistent, many of them have been extensively benchmarked in the past years by our group[14−17] and others,[18−26] addressing the quantification of errors for each method for vertical excitation energies, transition moments, and potential energy surfaces. In a recent study by our group,[15] the popular CC2 method[7] was found to perform very badly for Rydberg-type excited states, despite being accurate for the valence-type ones. Subsequently, our investigation[16] found that the latter should rather be regarded as a result of fortuitous error cancellation, which does not occur for the Rydberg states. Recently, we also found[17] that the accuracy observable for the vertical excitation energies of valence states does not extend to the associated surfaces and energy derivatives either. The CC2 level excited state gradients and surface plots that follow these forces showed a surprisingly bad performance when compared to high-level reference data for many states where otherwise a very good vertical excitation energy is obtained.

Since, however, a cost-effective and reliable CC method is highly demanded, it is reasonable to investigate various modifications of CC2 theory that may offer better accuracy. One of such modifications is the introduction of spin-component-scaling by Grimme and co-workers[27,28] which was found to slightly reduce the errors for excited state bond distances and adiabatic excitation energies of small inorganic molecules by Hellweg et al.,[29] as well as the error of 0−0 transitions for a large set of organic molecules by Winter et al.[30] These studies, however, did not focus on situations where CC2 shows a subpar performance, and thus, the improvements relative to regular CC2 were less significant.

In this study, we investigate the performance of spin-component-scaled variants of CC2 using the methodology and test systems of refs 16 and 17. We benchmark the accuracy of vertical excitation energies of valence- and Rydberg-type states, as well as the gradients and potential energy surfaces (PES) of several excited states of some representative systems. As reference, we use high level *ab initio* data obtained by CC methods involving triple excitations: EOM-CCSDT,[31] EOM-CCSD(T)(a)*,[32] and CC3-LR.[8] This way, we aim to quantify

Received: July 8, 2019
Published: August 21, 2019

Table 1. Statistics on Relative Vertical Excitation Energies Compared to CC3-LR, in eV

			Valence states			Rydberg states			
Method	C_{os}	C_{ss}	Mean ΔE	$\sigma_{\Delta E}$	Max. $\lvert\Delta E\rvert$	Mean ΔE	$\sigma_{\Delta E}$	Max. $\lvert\Delta E\rvert$	Mean Δ(Valence−Rydberg)
	1.1	0.0	0.41	0.28	1.06	0.27	0.24	0.89	0.15
	1.1	1/3	0.26	0.18	0.62	0.02	0.14	0.49	0.23
	1.1	0.5	0.18	0.13	0.51	−0.10	0.14	0.47	0.27
	1.2	0.0	0.34	0.24	0.89	0.17	0.19	0.73	0.17
SCS-CC2	1.2	1/3	0.18	0.14	0.53	−0.07	0.14	0.48	0.24
	1.2	0.5	0.10	0.09	0.40	−0.19	0.18	0.51	0.29
SOS-CC2	1.3	0.0	0.26	0.20	0.71	0.08	0.16	0.56	0.18
	1.3	1/3	0.09	0.11	0.41	−0.16	0.17	0.52	0.26
	1.3	0.5	0.02	0.08	0.33	−0.29	0.23	0.61	0.30
CC2[a]			0.02	0.10	0.40	−0.38	0.26	0.68	0.40
EOM-CCSD(2)			0.26	0.20	0.69	0.13	0.12	0.31	0.13
EOM-CCSD			0.17	0.13	0.42	0.11	0.08	0.33	0.07

[a]Calculated without resolution of identity approximation.

the effect of spin-component scaling on the reliability and consistency of CC2, investigate the impact of the exact values of the spin-component scaling factors, and thereby address the ways to remedy the previously revealed flaws of CC2 while also retaining its attractive computational cost.

In the following section, we briefly present the concept of spin-component-scaled CC2 methods. (For a detailed review about spin-component-scaled models, the reader is advised to read the excellent review of Grimme and co-workers.[28]) Subsequently, we review the methodology and test systems of this study (the ones already used in refs 16 and 17, followed by the presentation of results for excitation energies, excited state gradients, and potential energy surfaces. The paper concludes with a discussion of the findings.

2. METHODS

2.1. Spin-Component-Scaled CC2 methods. The concept of spin-component scaling (SCS), i.e., the introduction of multiplicative constants for the parallel-spin and antiparallel-spin components of the energy expression, was originally proposed by Grimme[27] for second-order Møller−Plesset perturbation theory (MP2) and by Jung et al.[33] with the presentation of the scaled opposite-spin MP2 (SOS-MP2) method. The proposed empirical scaling factors $C_{\alpha\alpha}$ and $C_{\beta\beta}$ for the parallel-spin components of the SCS-MP2 energy were $C_{ss} = 1/3$, while for the antiparallel part a value of $C_{\alpha\beta} = C_{\beta\alpha} = C_{os} = 6/5$ has been suggested. These choices were later justified by Szabados,[34] who showed that they are close to what can be obtained with a two-parameter scaling of the zeroth order Hamiltonian satisfying Feenberg's minimal condition. In the SOS-MP2 method, C_{ss} is set to zero, while C_{os} is adjusted to 1.3. Neglecting the parallel-spin components entirely has the advantage that, if combined with the resolution of identity (RI) approximation, the computational scaling can be reduced to no more than the fourth power of the system size.[35]

The generalization of SCS and SOS to CC2 for ground and excited states was done by Hättig and co-workers.[29,35] More recently, Winter and Hättig reported the implementation of SOS-CC2 using the RI approximation that features the analytic evaluation of the excited state gradient.[36] The scaling factors $C_{\sigma\sigma'}$, with σ and σ' referencing α or β spins, are introduced into the CC2 energy expression

$$E_{SCS-CC2} = \langle HF|\tilde{H} + \sum_{\sigma\sigma'} C_{\sigma\sigma'}[\tilde{H}, \hat{T}_2^{\sigma\sigma'}]|HF\rangle \quad (1)$$

where $\tilde{H}$ is the $\hat{T}_1$-transformed Hamiltonian $\tilde{H} = \exp(-\hat{T}_1)\hat{H}\exp(\hat{T}_1)$ and $\hat{T}_2^{\sigma\sigma'}$ refers to the double excitation cluster operator

$$\hat{T}_2^{\sigma\sigma'} = \sum_{iajb} t_{ij}^{ab} \hat{a}_{a,\sigma'}^{\dagger}\hat{a}_{b,\sigma}^{\dagger}\hat{a}_{j,\sigma'}\hat{a}_{i,\sigma} \quad (2)$$

with $\hat{a}^{\dagger}$ and $\hat{a}$ being creation and annihilation operators, respectively, on occupied orbitals i, j and virtual orbitals a, b. The same scaling factors are applied in the equations determining the ground state singles amplitudes. The vertical excitation energies are obtained from the diagonalization of the CC2 Jacobian matrix $\mathbf{A}$

$$A = \begin{pmatrix} \mathbf{A}_{SS} & \mathbf{A}_{SD} \\ \mathbf{A}_{DS} & \mathbf{A}_{DD} \end{pmatrix} = \left(\begin{array}{c|c} \langle \mathbf{S}\left|\left[\left(\tilde{H} + \sum_{\sigma\sigma'} C_{\sigma\sigma'}\left[\tilde{H}, \hat{T}_2^{\sigma\sigma'}\right]\right), \hat{\tau}_1\right]\right|HF\rangle & \langle \mathbf{S}\left|C_{\sigma\sigma'}\left[\tilde{H}, \hat{\tau}_2^{\sigma\sigma'}\right]\right|HF\rangle \\ \hline \langle \mathbf{D}\left|\left[\tilde{H}, \hat{\tau}_1\right]\right|HF\rangle & \mathbf{A}_{DD}, \end{array}\right) \quad (3)$$

with $\hat{\tau}_1$ and $\hat{\tau}_2$ representing the set of single and double excitation operators, and $\mathbf{S}$ and $\mathbf{D}$ referencing the manifold of singly and doubly excited determinants with respect to the Hartree−Fock determinant $|HF\rangle$, respectively. If canonical molecular orbitals are used, the doubles−doubles block $\mathbf{A}_{DD}$ is diagonal, with the diagonal elements being the orbital energy differences $\varepsilon_{aibj} = \varepsilon_a - \varepsilon_i + \varepsilon_b - \varepsilon_j$. Implementations of the spin-component-scaled CC2 variants are now available in many known computer codes, including TURBOMOLE[35−37] and MRCC.[38−40]

2.2. Excited State Gradients. Geometrical first derivatives of the excited state electronic energy at the ground state equilibrium geometry (also referred to as the Franck−Condon gradient) can be obtained analytically or numerically. For the former approach, implementations are available at CC2,[7,41] as well as its spin-component-scaled versions SCS-CC2[29] and SOS-CC2[35,36] in the TURBOMOLE,[37] and at CC2, CCSD[42,43] and CCSDT[44,45] levels in the CFOUR[46] program packages, while for the CCSD(T)(a)* method of Matthews and Stanton[32] numerical gradients are used here. These latter calculations tend to be very expensive if the molecule has many internal degrees of freedom and several excited states are investigated.

Gradient vectors obtained with different methods can be compared by evaluating their length and direction by

DOI: 10.1021/acs.jctc.9b00676
J. Chem. Theory Comput. 2019, 15, 5523−5531

Table 2. Vertical Excitation Energies, Length, and Angle of Excited State Gradient Vectors of Methanimine

	Excitation energy (ev)	Gradient length (au)	Angles (deg)				
			SCS-CC2	SOS-CC2	CC2	CCSD	CCSDT
			State 1 (n–π^*)				
SCS-CC2	5.73	0.1636	0.00	0.25	0.51	3.11	1.56
SOS-CC2	5.78	0.1641		0.00	0.76	3.07	1.58
CC2	5.65	0.1626			0.00	3.33	1.56
CCSD	5.54	0.1576				0.00	4.37
CCSDT	5.47	0.1692					0.00
			State 2 (σ–π^*)				
SCS-CC2	10.01	0.2543	0.00	0.63	1.37	4.92	6.37
SOS-CC2	10.05	0.2518		0.00	2.00	5.02	6.50
CC2	9.92	0.2606			0.00	4.74	6.12
CCSD	9.79	0.2423				0.00	3.18
CCSDT	9.65	0.2387					0.00

numerical measures. As for the latter, the angle of two vectors **a** and **b** is defined as

$$\gamma = \cos^{-1}\left(\frac{\mathbf{ab}}{\|\mathbf{a}\|\cdot\|\mathbf{b}\|}\right) \tag{4}$$

which together with the gradient norms provides a convenient measure of similarity.[17]

2.3. Surface Plots Following Franck–Condon Forces. Immediately after being excited to the state of interest, the system is likely to follow a path marked by the Franck–Condon gradient. Altering the geometry in a stepwise manner in the direction of these forces with steps proportional to the gradient thus explores an important region of the PES.[17] The points of the function

$$E_n^i = E^i[\mathbf{R}_0 - n\cdot S\cdot(\bar{\nabla}E^i)_{\mathbf{R}_0}] - E^0[\mathbf{R}_0] \tag{5}$$

can be obtained for the states of interest, where $E^i[\mathbf{R}]$ is the total electronic energy of state i at geometry $\mathbf{R}$, $\bar{\nabla}E^i$ refers to the mass-weighted gradient of this state, and $\mathbf{R}_0$ is the ground state equilibrium geometry. The step size S was chosen as $0.6 m_u^{1/2} E_h^{-1} a_0^2$, as it was proven to be a well-working value in our previous study.[17] The parallelity of these curves can illustrate the differences between methods, highlighting their impact on the quality of the PES. The comparison of these plots for lower level methods can be done by investigating their "divergence" from a reference curve

$$\bar{E}_n^i = E_n^i - E_n^{i,ref} - (E_0^i - E_0^{i,ref}) \tag{6}$$

where the second term shifts the curve to 0 for $n = 0$.

2.4. Test Systems. The accuracy of vertical excitation energies was evaluated on a subset of the benchmark set used in ref 16, i.e., low-lying excited states of small- and medium-sized molecules with an extended π system. It forms a representative large subset of the benchmark set of Thiel et al.,[18] the elements chosen with the objective that all states could be reliably calculated with all methods investigated in this study. As reference, the linear response CC3 values from ref 16 were used, which had been found very accurate in earlier works.[14−16] Altogether, the excitation energies of 64 valence and 56 Rydberg states were obtained with various spin-component-scaled CC2 variants: the regular SCS-CC2 (C_{os} = 1.2, C_{ss} = 1/3) and SOS-CC2 (C_{os} = 1.3, C_{ss} = 0), as well as ones with different choices of C_{os} (1.1, 1.2, and 1.3) and C_{ss} (0.0, 1/3, and 1/2). The aug-cc-pVDZ basis set of Dunning et al.[47] was employed in all cases.

For the evaluation of gradients and surfaces, the systems and electronic states of our previous study[17] were investigated with SCS methods. That is, the benchmark set consisted of low-lying valence excited states of four small- and medium-sized systems that contain π-bonds and nitrogen heteroatoms: methanimine (formaldimine), formamide, cytosine, and guanine. As reference, very accurate CCSDT results were used, except in the case of guanine, where the CCSD(T)(a)* values have been used instead. This latter method was found to be very accurate and consistent in earlier benchmarks, outperforming even CC3 in many cases.[17] In these calculations, the states under investigation being of pure valence type, cc-pVDZ basis set of Dunning et al.[48] was employed.

The spin-component-scaled CC2 calculations were performed using the TURBOMOLE[37] program system with the use of resolution of identity (RI) approximation and core electrons excluded from the correlation treatment. For the CC2, CCSD, CCSD(T)(a)*, and CCSDT calculations, the CFOUR[46] program package has been used, and the RI approximation was not invoked. The reference structures were optimized at the CCSD/cc-pVDZ level.[17]

3. RESULTS

3.1. Vertical Excitation Energies. Statistics on the error of the vertical excitation energies are presented in Table 1 for the different spin-component-scaled CC2 variants as well as for the regular CC2, CCSD(2), and CCSD methods, evaluated against the CC3 reference values. (The full set of results for the excitation energies is available in the Supporting Information.) The latter two doubles methods, as already shown in ref 16, have a general tendency to slightly overestimate the vertical excitation energy of both valence and Rydberg states. CC2, while being very accurate for valence type states, underestimates the Rydberg excitation energies by nearly 0.4 eV. This misbalance, evaluated as the difference of mean errors for the valence and Rydberg set, is shown in the last column of Table 1. One can see that the misbalance is significantly reduced for all spin-component-scaled variants, down to as low as 0.15 eV for C_{os} = 1.1 and C_{ss} = 0.0. SOS-CC2 (C_{os} = 1.3, C_{ss} = 0) shows 0.18 eV, while the $C_{ss} \neq 0$ variants give considerably higher values up to 0.3 eV.

DOI: 10.1021/acs.jctc.9b00676
J. Chem. Theory Comput. 2019, 15, 5523−5531

Table 3. Vertical Excitation Energies, Length, and Angle of Excited State Gradient Vectors of Formamide

			Angles (deg)				
	Excitation energy (eV)	Gradient length (au)	SCS-CC2	SOS-CC2	CC2	CCSD	CCSDT
			State 1 ($n-\pi^*$)				
SCS-CC2	6.05	0.3010	0.00	0.47	0.89	5.44	4.90
SOS-CC2	6.03	0.2986		0.00	1.36	5.27	4.75
CC2	6.00	0.3061			0.00	5.85	5.26
CCSD	5.87	0.2678				0.00	1.13
CCSDT	5.84	0.2850					0.00
			State 2 ($\pi-\pi^*$)				
SCS-CC2	8.05	0.2196	0.00	8.35	22.59	2.10	8.07
SOS-CC2	8.01	0.2265		0.00	30.94	9.54	15.92
CC2	7.71	0.2370			0.00	21.63	16.00
CCSD	7.92	0.1975				0.00	6.87
CCSDT	7.64	0.2066					0.00

Table 4. Vertical Excitation Energies, Length, and Angle of Excited State Gradient Vectors of Cytosine

			Angles (deg)				
	Excitation energy (eV)	Gradient length (au)	SCS-CC2	SOS-CC2	CC2	CCSD	CCSDT
			State 1 ($\pi-\pi^*$)				
SCS-CC2	5.06	0.2354	0.00	2.87	5.75	6.71	3.18
SOS-CC2	5.10	0.2316		0.00	8.61	4.90	5.51
CC2	4.96	0.2467			0.00	11.76	4.44
CCSD	5.11	0.2034				0.00	8.08
CCSDT	4.86	0.2267					0.00
			State 2 ($\pi-\pi^*$)				
SCS-CC2	6.05	0.2203	0.00	2.46	4.55	7.90	8.73
SOS-CC2	6.14	0.2203		0.00	7.00	7.92	10.36
CC2	5.86	0.2171			0.00	9.96	7.24
CCSD	6.10	0.1961				0.00	7.73
CCSDT	5.75	0.2095					0.00
			State 3 ($n-\pi^*$)				
SCS-CC2	5.52	0.1706	0.00	10.40	36.49	19.49	5.83
SOS-CC2	5.65	0.1645		0.00	46.03	10.63	14.13
CC2	5.15	0.2489			0.00	54.91	35.46
CCSD	5.53	0.1538				0.00	21.45
CCSDT	5.28	0.1628					0.00

On the other hand, decreasing C_{ss} deteriorates the accuracy of the vertical excitation energy of valence states, shifting them up by up to 0.41 eV (C_{os} = 1.1, C_{ss} = 0) from the reference. The Rydberg states are also up-shifted as C_{ss} approaches zero, certain values (C_{os} = 1.1, C_{ss} = 1/3) giving a mean error as low as 0.02 eV. With decreasing C_{os}, a similar tendency is observed with both valence and Rydberg states shifted upward. Although no particular choice of C_{ss} and C_{os} clearly stands out from the evaluated variants, the SOS-CC2 (C_{os} = 1.3, C_{ss} = 0.0) shows a remarkable consistency with a mean error for the Rydberg states as low as 0.08 eV and 0.26 eV for the valence states, same as the much more expensive CCSD(2) method. Even the respective standard deviations are in line with those of CCSD(2), which are, however, still much larger than those of CCSD. The same holds for the valence−Rydberg misbalance of 0.18 eV; nevertheless, this value seems very acceptable compared to CC2.

3.2. Franck−Condon Gradients. Franck−Condon gradients evaluated according to eq 4 are shown in Tables 2, 3, 4, and 5. For the two considered valence excited states of the methanimine (formaldimine) molecule, which are of $n - \pi^*$ and $\sigma - \pi^*$ type, respectively, the spin-component-scaled gradients show little difference to CC2, but have a consistently more accurate length. For the first, $n - \pi^*$ excited state of formamide, the CC2 gradient is as much as 5.26 degrees askew from CCSDT, while the SCS and SOS variants show a minor improvement with 4.90 and 4.75 degrees. The error of the vector length is also reduced by 24 and 36%, respectively. A much larger effect is observed for the other, $\pi - \pi^*$ state, where the significant directional inaccuracy of the CC2 gradient (16.00 degrees) is reduced to half (8.07 degrees) with the regular SCS scheme, but to no less than 15.92 degrees with SOS-CC2. The gradient norms also show improvement, with the SCS-CC2 one being almost in line with the CCSD result.

In the case of cytosine, the $\pi-\pi^*$ states remain generally well described by all doubles methods. For the first state, SCS-CC2 gives an excellent gradient direction, while also reducing the error of the CC2 gradient length by nearly 60%. As for the latter, the SOS-CC2 result is even better, practically as

DOI: 10.1021/acs.jctc.9b00676
J. Chem. Theory Comput. 2019, 15, 5523−5531

Table 5. Vertical Excitation Energies, Length, and Angle of Excited State Gradient Vectors of Guanine

			Angles (deg)				
	Excitation energy (eV)	Gradient length (au)	SCS-CC2	SOS-CC2	CC2	CCSD	CCSD(T)(a)*
			State 1 ($\pi-\pi^*$)				
SCS-CC2	5.38	0.1947	0.00	1.46	3.85	8.73	4.08
SOS-CC2	5.40	0.1938		0.00	5.23	7.94	3.91
CC2	5.35	0.1982			0.00	11.44	6.39
CCSD	5.44	0.1697				0.00	6.60
CCSD(T)(a)*	5.32	0.1843					0.00
			State 2 ($\pi-\pi^*$)				
SCS-CC2	6.03	0.2062	0.00	2.32	4.34	7.66	3.98
SOS-CC2	6.11	0.2070		0.00	6.57	7.87	5.10
CC2	5.88	0.2077			0.00	9.35	4.94
CCSD	6.11	0.1798				0.00	6.55
CCSD(T)(a)*	5.91	0.1957					0.00
			State 3 ($\pi-\pi^*$)				
SCS-CC2	7.02	0.1771	0.00	2.30	3.96	10.33	5.88
SOS-CC2	7.07	0.1732		0.00	5.92	10.94	7.21
CC2	6.91	0.1843			0.00	11.90	6.57
CCSD	7.10	0.1498				0.00	6.04
CCSD(T)(a)*	6.87	0.1788					0.00
			State 4 ($n-\pi^*$)				
SCS-CC2	5.87	0.3024	0.00	1.96	5.11	4.99	1.63
SOS-CC2	5.92	0.2979		0.00	7.02	3.95	2.55
CC2	5.75	0.3173			0.00	9.11	5.21
CCSD	5.80	0.2626				0.00	4.94
CCSD(T)(a)*	5.75	0.2835					0.00
			State 5 ($n-\pi^*$)				
SCS-CC2	6.84	0.1782	0.00	7.99	26.37	31.21	22.20
SOS-CC2	6.94	0.1699		0.00	31.33	24.30	15.70
CC2	6.57	0.2339			0.00	47.84	38.52
CCSD	6.87	0.1705				0.00	11.90
CCSD(T)(a)*	6.73	0.1823					0.00

accurate as CCSD. For the second $\pi-\pi^*$ state, the spin-component-scaled gradients do not outperform the CC2 ones, although the changes remain minor both in the vector length and its direction. For the third $n-\pi^*$ state, a disastrous performance of CC2 was found earlier.[17] Thankfully, the spin-component-scaled variants seem to correct this behavior to a remarkable extent: both the SCS-CC2 and SOS-CC2 gradients are better than even CCSD, the former having a directional error as little as 5.83°, compared to 35.46° in the case of CC2. The vector is no more than 4.79% longer than the CCSDT reference, while the SOS-CC2 one is even better, with an error as low as 1%.

For guanine, where the CCSD(T)(a)* method was introduced as a reference in our previous study,[17] a similar tendency can be observed for the three $\pi-\pi^*$ states as well as for the first $n-\pi^*$ one: the spin-component-scaled techniques outperform both CC2 and CCSD in the accuracy of the gradient length and in the case of SCS-CC2 even in its direction in all cases. As for the second $n-\pi^*$ state, the dramatic error of the CC2 gradient is greatly reduced by spin-component scaling. The SOS-CC2 vector is only 15.70° askew from the reference, compared to 38.52° for CC2, and even SCS-CC2 has a 16° smaller error than CC2. The SCS-CC2 gradient vector is no more than 2% shorter than the CCSD(T)(a)* one, representing a huge improvement over CC2 which overshoots the vector by more than 28%.

3.3. Surface Plots. The surface plots following Franck–Condon forces defined by eqs 5 and 6 are presented for the investigated states on the left and right panels of Figures 1, 2, 3, and 4, respectively. For the two smallest systems, the above-mentioned improvement of spin-component scaling techniques over CC2 is well shown by these curves as well. With the exception of the lowest, $n-\pi^*$ state of formaldimine where all doubles techniques deliver excellent accuracy, the SCS-CC2 and SOS-CC2 results fall between CC2 and CCSD, always giving a smaller divergence from the reference than CC2. In the case of formamide, SCS-CC2 outperforms even CCSD in the accuracy of the surface. In the most critical $\pi-\pi^*$ state, it seems safe to say that the tremendous inaccuracy of CC2 is essentially eliminated by the introduction of spin-component scaling. The two SCS variants show a similar behavior for all states; the superiority of SCS-CC2 over SOS-CC2 is only pronounced in the case of formamide.

For the first excited state of cytosine, the intermediate nature of the SCS and SOS results between CC2 and CCSD is again recognizable. The accuracy relative to CCSDT is excellent, with the divergence never exceeding 0.1 eV along the entire surface scan. For SOS-CC2, it remains below 0.05

DOI: 10.1021/acs.jctc.9b00676
J. Chem. Theory Comput. 2019, 15, 5523−5531

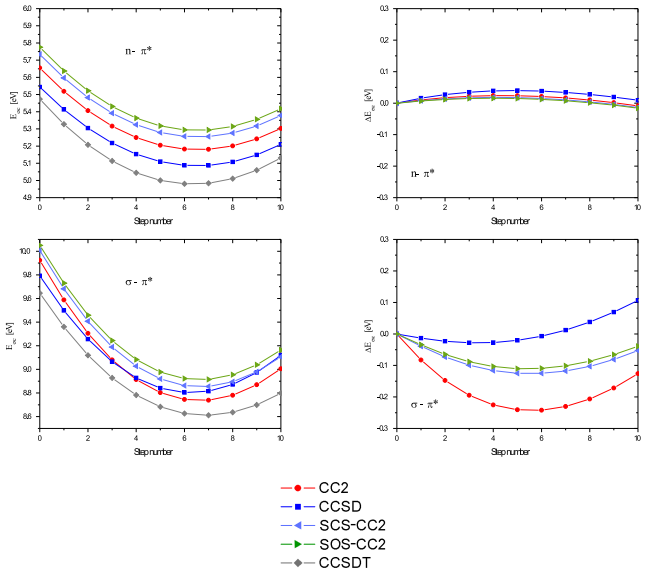

Figure 1. Potential energy curves following the gradient of low-lying excited states of methanimine relative to the ground state equilibrium energy (left panels) and their divergence from the respective CCSDT curve (right panels).

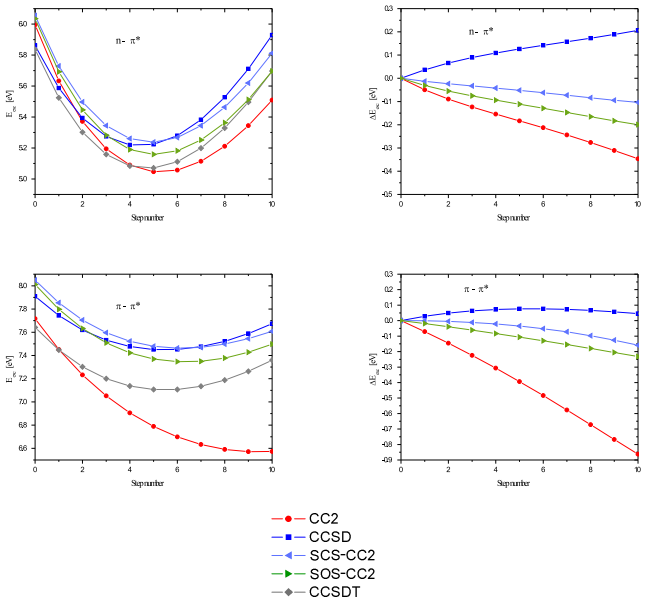

Figure 2. Potential energy curves following the gradient of low-lying excited states of formamide relative to the ground state equilibrium energy (left panels) and their divergence from the respective CCSDT curve (right panels).

eV. For the second $\pi-\pi^*$ state, all doubles methods work very well, and the spin-component-scaled variants seem to be more in line with CC2. The complete opposite is, however, observed for the $n-\pi^*$ state, where SCS-CC2 and SOS-CC2 are essentially in line with CCSD, while CC2 shows its catastrophic behavior found earlier[17] diverging from the reference by more than 1 eV.

For the $\pi-\pi^*$ states of guanine, we see a clear superiority of SCS methods over CCSD and, with the exception of the second state, over CC2 as well. The similarity of the SCS and SOS variants is remarkable, especially in the first few points of the scan. For the $n-\pi^*$ states, where the results are much

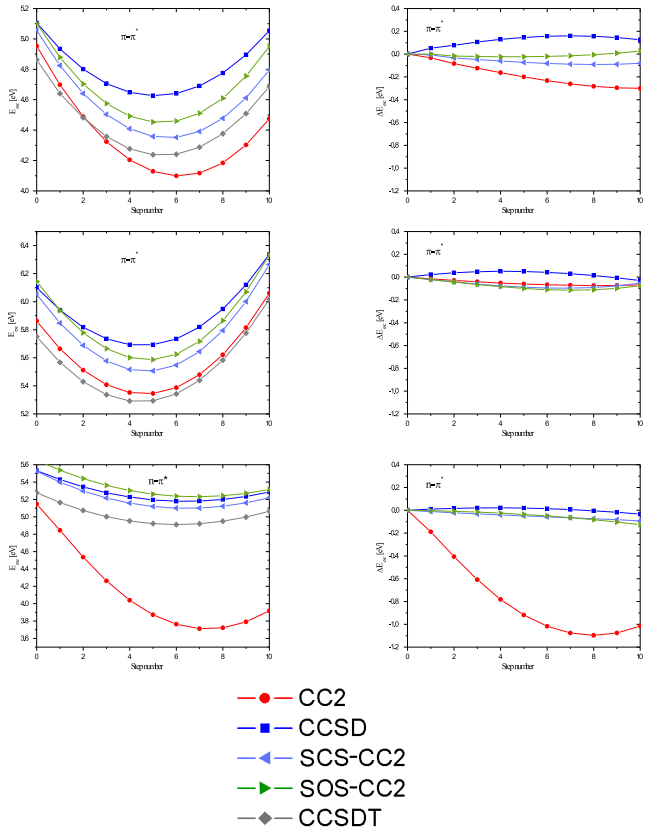

Figure 3. Potential energy curves following the gradient of low-lying excited states of cytosine relative to the ground state equilibrium energy (left panels) and their divergence from the respective CCSDT curve (right panels).

more controversial for approximate methods,[17] the picture is mixed: for the first state, the SCS-CC2 and SOS-CC2 curves exhibit a bad behavior similar to CC2. Yet their error, as shown by the divergence plots, is considerably smaller. For the second state, on the other hand, the SCS methods do not show the scary discrepancy of CC2, rather a very reasonably looking surface which is in the case of SCS-CC2 nearly as accurate as CCSD.

4. DISCUSSION AND CONCLUSIONS

The statistical findings on the accuracy of vertical excitation energies confirm that the valence−Rydberg misbalance of CC2 could be reduced by spin-component scaling, the biggest improvement in this aspect is seen when setting C_{ss} to zero. Since our recent study revealed that this problem of CC2 theory stems from the diagonal formulation of the doubles−doubles (DD) block of the Jacobian matrix $\mathbf{A}$,[16] this finding means that omitting parallel-spin terms from the other blocks of $\mathbf{A}$ compensates for this flaw of CC2 to a considerable extent. Although even the simple SOS-CC2 method performs well in this context, we could not find any variant that would be significantly better while also having low error for all types of states. In fact, we could not identify a clear optimum for the choice of C_{ss} and C_{os} for vertical excitation energies.

The other known discrepancy of CC2, the bad quality of potential energy surfaces in certain cases also seems to be largely remedied by spin-component scaling. Although both SCS-CC2 and SOS-CC2 represent a significant improvement over unscaled CC2 in the most problematic situations, the

DOI: 10.1021/acs.jctc.9b00676
J. Chem. Theory Comput. 2019, 15, 5523−5531

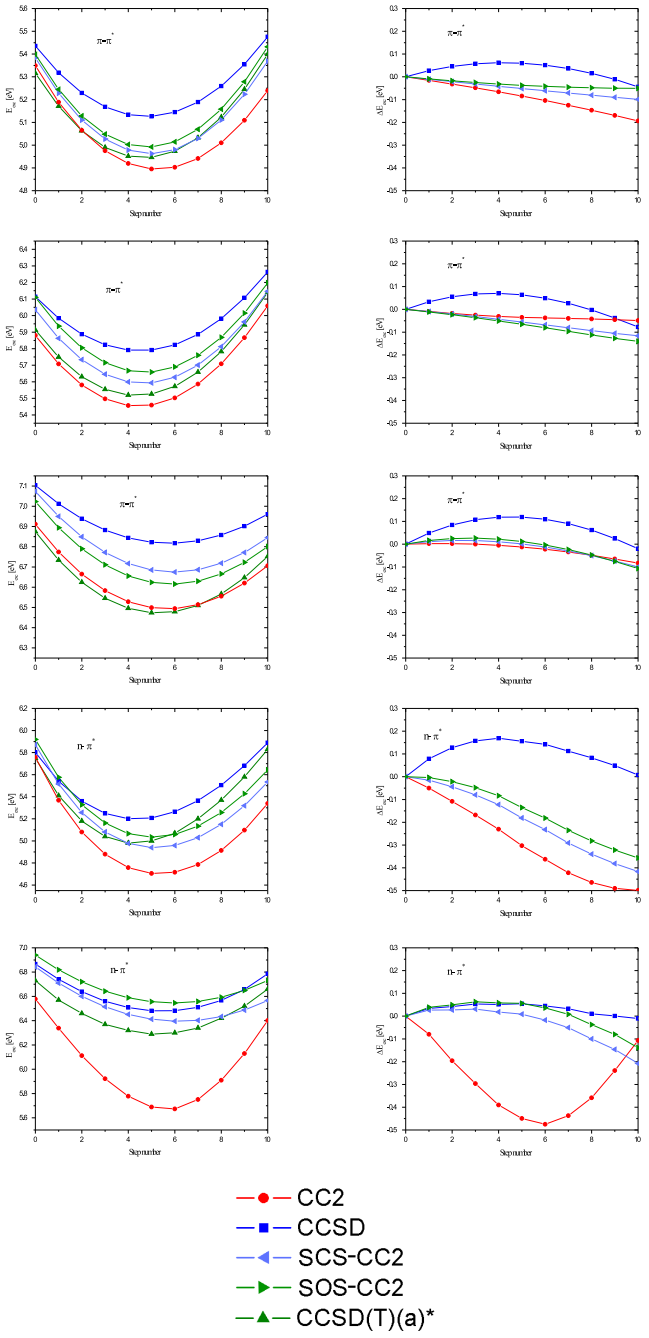

Figure 4. Potential energy curves following the gradient of low-lying excited states of guanine relative to the ground state equilibrium energy (left panels) and their divergence from the respective CCSD(T)(a)* curve (right panels).

overall results are still not of CCSD quality. Instead, the spin-component-scaled variants seem to reduce the large errors, giving results that fall between those of CCSD and CC2. SCS-CC2 and SOS-CC2 perform very similarly in these tests, so much that it is not possible the declare either being more accurate than the other.

Also considering, however, the computational costs, the SOS-CC2 variant whose implementations offer a scaling with the fourth power of the system size,[35,36] definitely seems a promising method for future applications. Despite the simplified formulation, the overall consistency and reliability are clearly better than that of regular CC2, which we think should be given a higher priority than the somewhat larger mean error of valence excitation energies. The latter is still in line with CCSD(2) and not far from that of CCSD, while the Rydberg states are described with a remarkably good accuracy.

Our results thus encourage the choice of spin-component-scaled variants in situations where the standard CC2 or ADC(2) methods would normally be used. Specifically, the computationally attractive C_{ss} = 0 versions seem powerful tools for applications on larger systems, studies we hope to see many more of in the future.

■ ASSOCIATED CONTENT

Supporting Information

The Supporting Information is available free of charge on the ACS Publications website at DOI: 10.1021/acs.jctc.9b00676.

Singlet valence and Rydberg excitation energies that form the benchmark set of this study. (PDF)

■ AUTHOR INFORMATION

Corresponding Authors

*E-mail: tat@chem.elte.hu (A.T.).
*E-mail: szalay@chem.elte.hu (P.G.S.).

ORCID

Attila Tajti: 0000-0002-7974-6141
Péter G. Szalay: 0000-0003-1885-3557

Notes

The authors declare no competing financial interest.

■ ACKNOWLEDGMENTS

This work has been supported by the National Research, Innovation and Development Fund (NKFIA), Grant No. 124293.

■ REFERENCES

(1) Sekino, H.; Bartlett, R. J. A Linear Response, Coupled-Cluster Theory for ExcitationEnergy. *Int. J. Quantum Chem.* **1984**, *26*, 255−265.
(2) Stanton, J. F.; Bartlett, R. J. The Equation of Motion Coupled-Cluster Method - A Systematic Biorthogonal Approach to Molecular-Excitation Energies, TransitionProbabilities, and Excited-State Properties. *J. Chem. Phys.* **1993**, *98*, 7029−7039.
(3) Comeau, D. C.; Bartlett, R. J. The Equation-of-Motion Coupled-Cluster Method - Applications to Open-Shell and Closed-Shell Reference States. *Chem. Phys. Lett.* **1993**, *207*, 414−423.
(4) Monkhorst, H. J. Calculation of Properties with Coupled-Cluster Method. *Int. J. Quantum Chem.* **1977**, *12*, 421−432.
(5) Koch, H.; Jørgensen, P. Coupled cluster response functions. *J. Chem. Phys.* **1990**, *93*, 3333.
(6) Koch, H.; Jensen, H. J. A.; Jørgensen, P.; Helgaker, T. Excitation energies from the coupled cluster singles and doubles linear response function (CCSDLR). Applications to Be, CH+, CO, and H2O. *J. Chem. Phys.* **1990**, *93*, 3345−3350.
(7) Christiansen, O.; Koch, H.; Jørgensen, P. The Second-order Approximate Coupled-Cluster Singles and Doubles Model CC2. *Chem. Phys. Lett.* **1995**, *243*, 409−418.
(8) Christiansen, O.; Koch, H.; Jørgensen, P. Response Functions in the CC3 Iterative Triple Excitation Model. *J. Chem. Phys.* **1995**, *103*, 7429−7441.
(9) Bartlett, R. J. Coupled-cluster approach to molecular structure and spectra: a step toward predictive quantum chemistry. *J. Phys. Chem.* **1989**, *93*, 1697−1708.
(10) Gauss, J. Coupled-Cluster Theory. In *Encyclopedia of Computational Chemistry*; 1998, p 615.

(11) Bartlett, R. J.; Musial, M. Coupled-cluster theory in quantum chemistry. *Rev. Mod. Phys.* **2007**, *79*, 291−352.
(12) Stanton, J. F.; Gauss, J. Perturbative Treatment of the Similarity Transformed Hamiltonian In Equation-of-Motion Coupled-Cluster Approximations. *J. Chem. Phys.* **1995**, *103*, 1064−1076.
(13) Gwaltney, S. R.; Nooijen, M.; Bartlett, R. J. Simplified methods for equation-of-motion coupled-cluster excited state calculations. *Chem. Phys. Lett.* **1996**, *248*, 189−198.
(14) Kánnár, D.; Szalay, P. G. Benchmarking Coupled Cluster Methods on Valence Singlet Excited States. *J. Chem. Theory Comput.* **2014**, *10*, 3757−3765.
(15) Kánnár, D.; Tajti, A.; Szalay, P. G. Accuracy of Coupled Cluster excitation energies in diffuse basis sets. *J. Chem. Theory Comput.* **2017**, *13*, 202−209.
(16) Tajti, A.; Szalay, P. G. Investigation of the Impact of Different Terms in the Second Order Hamiltonian on Excitation Energies of Valence and Rydberg States. *J. Chem. Theory Comput.* **2016**, *12*, 5477−5482.
(17) Tajti, A.; Stanton, J. F.; Matthews, D. A.; Szalay, P. G. Accuracy of Coupled Cluster Excited State Potential Energy Surfaces. *J. Chem. Theory Comput.* **2018**, *14*, 5859−5869.
(18) Schreiber, M.; Silva, M. R. J.; Sauer, S. P. A.; Thiel, W. Benchmarks for electronically excited states: CASPT2, CC2, CCSD, and CC3. *J. Chem. Phys.* **2008**, *128*, 134110.
(19) Sauer, S. P. A.; Schreiber, M.; Silva-Junior, M. R.; Thiel, W. Benchmarks for Electronically Excited States: A Comparison of Noniterative and Iterative Triples Corrections in Linear Response Coupled Cluster Methods: CCSDR(3) versus CC3. *J. Chem. Theory Comput.* **2009**, *5*, 555−564.
(20) Silva-Junior, M. R.; Sauer, S. P. A.; Schreiber, M.; Thiel, W. Basis set effects on coupled cluster benchmarks of electronically excited states: CC3, CCSDR (3) and CC2. *Mol. Phys.* **2010**, *108*, 453−465.
(21) Jacquemin, D.; Duchemin, I.; Blase, X. 0−0 Energies Using Hybrid Schemes: Benchmarks of TD-DFT, CIS(D), ADC(2), CC2, and BSE/ GWformalisms for 80 Real-Life Compounds. *J. Chem. Theory Comput.* **2015**, *11*, 5340−5359.
(22) Piecuch, P.; Hansen, J. A.; Ajala, A. O. Benchmarking the completely renormalised equation-of-motion coupled-cluster approaches for vertical excitation energies. *Mol. Phys.* **2015**, *113*, 3085−3127.
(23) Sous, J.; Goel, P.; Nooijen, M. Similarity transformed equation of motion coupled cluster theory revisited: a benchmark study of valence excited states. *Mol. Phys.* **2014**, *112*, 616−638.
(24) Huntington, L. M. J.; Demel, O.; Nooijen, M. Benchmark Applications of Variations of Multireference Equation of Motion Coupled-Cluster Theory. *J. Chem. Theory Comput.* **2016**, *12*, 114−132.
(25) Rishi, V.; Perera, A.; Nooijen, M.; Bartlett, R. J. Excited states from modified coupled cluster methods: Are they any better than EOM CCSD? *J. Chem. Phys.* **2017**, *146*, 144104.
(26) Harbach, P. H. P.; Wormit, M.; Dreuw, A. The third-order algebraic diagrammatic construction method (ADC(3)) for the polarization propagator for closed-shell molecules: Efficient implementation and benchmarking. *J. Chem. Phys.* **2014**, *141*, No. 064113.
(27) Grimme, S. Improved second-order Møller−Plesset perturbation theory by separate scaling of parallel- and antiparallel-spin pair correlation energies. *J. Chem. Phys.* **2003**, *118*, 9095−9102.
(28) Grimme, S.; Goerigk, L.; Fink, R. F. Spin-component-scaled electron correlation methods. *Wiley Interdisciplinary Reviews: Computational Molecular Science* **2012**, *2*, 886−906.
(29) Hellweg, A.; Grün, S. A.; Hättig, C. Benchmarking the performance of spin-component scaled CC2 in ground and electronically excited states. *Phys. Chem. Chem. Phys.* **2008**, *10*, 4119−4127.
(30) Winter, N. O. C.; Graf, N. K.; Leutwyler, S.; Hättig, C. Benchmarks for 0−0 transitions of aromatic organic molecules: DFT/B3LYP, ADC(2), CC2, SOS-CC2 and SCS-CC2 compared to high-resolution gas-phase data. *Phys. Chem. Chem. Phys.* **2013**, *15*, 6623−6630.
(31) Kucharski, S. A.; Wloch, M.; Musial, M.; Bartlett, R. J. Coupled-cluster theory for excited electronic states: The full equation-of-motion coupled-cluster single, double, and triple excitation method. *J. Chem. Phys.* **2001**, *115*, 8263−8266.
(32) Matthews, D. A.; Stanton, J. F. A new approach to approximate equation-of-motion coupled cluster with triple excitations. *J. Chem. Phys.* **2016**, *145*, 124102.
(33) Jung, Y.; Lochan, R. C.; Dutoi, A. D.; Head-Gordon, M. Scaled opposite-spin second order Møller−Plesset correlation energy: An economical electronic structure method. *J. Chem. Phys.* **2004**, *121*, 9793−9802.
(34) Szabados, A. Theoretical interpretation of Grimme's spin-component-scaled second order Møller−Plesset theory. *J. Chem. Phys.* **2006**, *125*, 214105.
(35) Winter, N. O. C.; Hättig, C. Scaled opposite-spin CC2 for ground and excited states with fourth order scaling computational costs. *J. Chem. Phys.* **2011**, *134*, 184101.
(36) Winter, N. O. C.; Hättig, C. Quartic scaling analytical gradients of scaled opposite-spin CC2. *Chem. Phys.* **2012**, *401*, 217.
(37) *TURBOMOLE V7.3 2018*, a development of University of Karlsruhe and Forschungszentrum Karlsruhe GmbH, 1989−2007, TURBOMOLE GmbH, since 2007. http://www.turbomole.com (accesed August 2019).
(38) MRCC, a quantum chemical program suite written by M. Kállay, P. R. Nagy, Z. Rolik, D. Mester, G. Samu, J. Csontos, J. Csóka, B. P. Szabó, L. Gyevi-Nagy, I. Ladjánszki, L. Szegedy, B. Ladóczki, K. Petrov, M. Farkas, P. D. Mezei, and B. Hégely. www.mrcc.hu. See also Rolik, Z; Szegedy, L; Ladjanszki, I; Ladoczki, B; Kallay, M An efficient linear-scaling CCSD(T) method based on local natural orbitals. *J. Chem. Phys.* **2013**, *139*, 094105.
(39) Mester, D.; Nagy, P. R.; Kállay, M. Reduced-cost linear-response CC2 method based on natural orbitals and natural auxiliary functions. *J. Chem. Phys.* **2017**, *146*, 194102.
(40) Mester, D.; Nagy, P. R.; Kállay, M. Reduced-cost second-order algebraic-diagrammatic construction method for excitation energies and transition moments. *J. Chem. Phys.* **2018**, *148*, No. 094111.
(41) Köhn, A.; Hättig, C. Analytic gradients for excited states in the coupled-cluster model CC2 employing the resolution-of-the-identity approximation. *J. Chem. Phys.* **2003**, *119*, 5021.
(42) Stanton, J. F. Many-Body Methods for Excited-State Potential-Energy Surfaces. 1. General-Theory of Energy Gradients for the Equation-of-Motion Coupled-Cluster Method. *J. Chem. Phys.* **1993**, *99*, 8840−8847.
(43) Stanton, J. F.; Gauss, J. Analytic Energy Gradients for the Equation-of-Motion Coupled-Cluster Method - Implementation and Application to the HCN/HNC System. *J. Chem. Phys.* **1994**, *100*, 4695−4698.
(44) Matthews, D. A.; Stanton, J. F. Non-orthogonal spin-adaptation of coupled cluster methods: A new implementation of methods including quadruple excitations. *J. Chem. Phys.* **2015**, *142*, 064108.
(45) Matthews, D. A.; Stanton, J. F. Accelerating the convergence of higher-order coupled cluster methods. *J. Chem. Phys.* **2015**, *143*, 204103.
(46) Stanton, J. F.; Gauss, J.; Cheng, L.; Harding, M. E.; Matthews, D. A.; Szalay, P. G. CFOUR, Coupled-Cluster Techniques for Computational Chemistry, a quantum-chemical program package. With contributions from A. A. Auer, R. J. Bartlett, U. Benedikt, C. Berger, D. E. Bernholdt, Y. J. Bomble, O. Christiansen, F. Engel, R. Faber, M. Heckert, O. Heun, M. Hilgenberg, C. Huber, T.-C. Jagau, D. Jonsson, J. Jusélius, T. Kirsch, K. Klein, W. J. Lauderdale, F. Lipparini, T. Metzroth, L. A. Mück, D. P. O'Neill, D. R. Price, E. Prochnow, C. Puzzarini, K. Ruud, F. Schiffmann, W. Schwalbach, C. Simmons, S. Stopkowicz, A. Tajti, J. Vázquez, F. Wang, J. D. Watts and the integral packages MOLECULE (J. Almlöf and P. R. Taylor), PROPS (P.R. Taylor), ABACUS (T. Helgaker, H. J. Aa. Jensen, P.

DOI: 10.1021/acs.jctc.9b00676
J. Chem. Theory Comput. 2019, 15, 5523−5531

Jørgensen, and J. Olsen), and ECP routines by A. V. Mitin and C. van Wüllen. For the current version, see http://www.cfour.de.
(47) Kendall, R. A.; Dunning, T. H., Jr.; Harrison, R. J. Electron-Affinities of the 1st-Row Atoms Revisited - Systematic Basis-Sets and Wave-Functions. *J. Chem. Phys.* **1992**, *96*, 6796−6806.
(48) Dunning, T. H., Jr. Gaussian basis sets for use in correlated molecular calculations. I. The atoms boron through neon and hydrogen. *J. Chem. Phys.* **1989**, *90*, 1007−1023.

DOI: 10.1021/acs.jctc.9b00676
J. Chem. Theory Comput. 2019, 15, 5523−5531